Two Dental Implants Designed for Immediate Loading: A Finite Element Analysis

Laurent Pierrisnard, DDS[1]/Guy Hure, DDS[2]/Michel Barquins, DSc[3]/Daniel Chappard, Dr Med[4]

Purpose: *The aim of this study was to evaluate by finite element analysis the influence of the design of 3 different dental implants on micromovements, cervical shearing stress intensity, and stress distribution after occlusal loading.* ***Materials and Methods:*** *The first investigated implant was a classical cylinder, the second was reinforced by 2 bicortical locking pins, and the third was an expanding dental implant. The parameters analyzed were the implant's geometry, the quality of the cancellous bone, and the orientation of occlusal loading.* ***Results:*** *It was found that initial stability of the locking pin implant was greater than the initial stability of the other investigated implant designs, regardless of the quality of cancellous bone and orientation of occlusal loading; in low-rigidity cancellous bone, under a horizontal load (500 N), decreasing displacement compared to those of the other investigated implants was 16 µm. The apical expansion and locking pin implants exhibited favorable behavior regarding the distribution and intensity of cervical shearing stresses; in low-rigidity cancellous bone, under horizontal load, decreasing cervical stresses compared with those of the cylindric implant were 10 MPa for the apical expansion implant and 150 MPa for the locking pin implant.* ***Discussion:*** *For the cylindric implant, stresses were concentrated in the neck region; for the apical expansion implant, stresses were evenly distributed from the neck to the apex of the implant. For the locking pin implant, stresses around the neck were moderate and appeared concentrated around the pins.* ***Conclusions:*** *Initial stability of the pin implant was greater than that of the expanding implant, but the expanding implant showed the most favorable stress distribution.* (INT J ORAL MAXILLOFAC IMPLANTS 2002;17:353–362)

Key words: *biomechanics, dental implants, dental stress analysis, finite element analysis*

Success with dental implant procedures largely depends on the presence of osseointegration. Brånemark's protocol includes 2 separate procedures. First, the implant is placed and submerged under a hermetically sutured mucosa to permit proper healing without risk of bacteremia in the absence of any functional solicitation. Second, the implant is uncovered, an abutment is attached, and if osseointegration has occurred, a restoration can be placed on the abutment. Several factors are involved in achieving osseointegration. They include metal composition,[1–3] suitable implant geometry,[1,4–6] absence of overheating during site preparation,[1,7–9] adequate bone quality,[10–12] and absence of loading during the healing period.[1,13]

To eliminate the important psychologic and functional handicap related to a 6- to 12-month healing period,[14] a 1-step surgical technique was proposed by the ITI International Team for Oral Implantology (Waldenburg, Switzerland) and has achieved comparable success rates.[10,15–19] This technique involves nonsubmerged implants, and loading usually starts earlier than in the Brånemark technique. However, immediate loading raises the problem of micromovement, which when it exceeds 100 µm[20,21] can induce fibrous tissue formation at the

[1]Associate Professor, Faculty of Dental Surgery, Montrouge, University of Paris V, Paris, France.
[2]Private Practice, Paris, France.
[3]Research Director, Centre National de la Recherche Scientifique (CNRS)-Ecole Supérieure de Physique et Chimie Industrielle (ESPCI), Paris, France.
[4]Professor, LHEA Laboratory Histology, Faculty of Medicine, University of Angers, Angers, France.

Reprint requests: Dr Laurent Pierrisnard, 133 rue Lamarck, 75018 Paris, France. Fax: +33 1 44 85 39 35.
E-mail: laurent.pierrisnard@wanadoo.fr

Table 1 Composition of the 3 implants

Element	Percent composition
Titanium	99.739
Iron	0.100
Oxygen	0.130
Carbon	0.020
Nitrogen	0.008
Hydrogen	0.003

bone-implant interface instead of the desired bone regeneration. Control of these micromovements is possible in long-span prosthodontic designs where several different implant abutments are rigidly bound together.[22–27] Adequate control is more hazardous with single-tooth replacements, which have been used more frequently in regular clinical practice.[28,29] This comparative mechanical study by finite element analysis (FEA) (linear elasticity) was intended to evaluate 2 commercially pure (cp) titanium implant systems designed to control micromovements after immediate loading, and to analyze the stress intensity and distribution generated throughout their structure. The 2 configurations investigated in the present study were an implant with a bicortical locking pin system and an expanding implant. A classical threaded cylindric implant served as a reference.

MATERIALS AND METHODS

Implants

All implants were made of cp titanium grade 2[30] (Table 1) and their dimensions were similar (diameter = 3.75 mm and length = 11.5 mm). A classical cylindric implant served as reference (Figs 1a and 1b). Two new configurations were investigated in the present study: *(1)* an implant with a bicortical locking pin system (Figs 2a and 2b), and *(2)* an expanding implant (Figs 3a and 3b). Design data were obtained from Euroteknika (Paris, France). Both configurations were designed to reduce micromovements generated through occlusal loading.

Finite Element Analysis

Calculation and visualization of stress, deformation, and displacement of complex structures under simulated forces were evaluated by FEA. Eight-nodal isoparametric brick elements (tridimensional models) were constructed by use of Cadsap-Algor (CADLM, Gif-sur-Yvette, France). In this study, all materials that were isotropic and reacted with linear elasticity were considered. This study did not take into account viscoelastic response of the bony structures to occlusal efforts. Nevertheless, the finite element method permits comparison of the influence of various parameters, such as geometric configurations of the implants.

The classical threaded cylindric implant served as a reference model (Figs 1a and 1b) and was compared to both the bicortical locking pin implant (Figs 2a and 2b) and the expanding implant (Figs 3a and 3b). To preserve simplicity, the prosthetic crown was not modeled. The abutment, screwed onto the implants, was identical for the 3 investigated designs and was put under 500-N loads. This intensity was chosen because it is the mean maximal force that the stomatognathic device is able to develop in the molar region.[31] The 3 modeled implants were placed in an osseous base (fragment of mandibular arch) made of a cortical bone envelope around cancellous bone (Figs 4a to 4c). The osseous base was considered to be totally embedded (boundary conditions). The link between the implant neck and the cortical bone can simulate clinical reality only if it is assumed that osseointegration (interfacial rigidity) has occurred in the region of the threads at the neck of the implant. Therefore, a virtual membrane (with a negligible width) was assumed around the implant neck, so as to limit interfacial rigidity while keeping the neck of the implant in intimate contact with the cortical bone (Fig 5).

The results were to be moderated given that it is impossible to quantify the difference, from a strictly mechanical point of view, between osseointegration and the immediate stability observed clinically. The investigated parameters were: geometry of the implant, quality of cancellous bone, and orientation of the occlusal load (axial force, oblique force at an angle of 45 degrees, and horizontal force at a right angle to the axial force). Concerning the locking pin implant, oblique and horizontal forces were applied following the buccolingual (BL) direction (ie, parallel to the pins), then following the mesiodistal (MD) direction (at a right angle to the pins). The method required that physical properties of the materials under study be introduced in the model: E, Young's modulus, and ν, Poisson's ratio. For titanium, the parameters have been validated in the literature (Table 2).[32] However, for bony structures, different values are available, but the most commonly used in the literature were inserted in the model.[33,34] The characteristics of cancellous bone are known to be dependent on bone micro-architecture, an important factor in bone quality, and bone quality stands out as the single greatest determinant in implant

Fig 1a Cylindric implant.

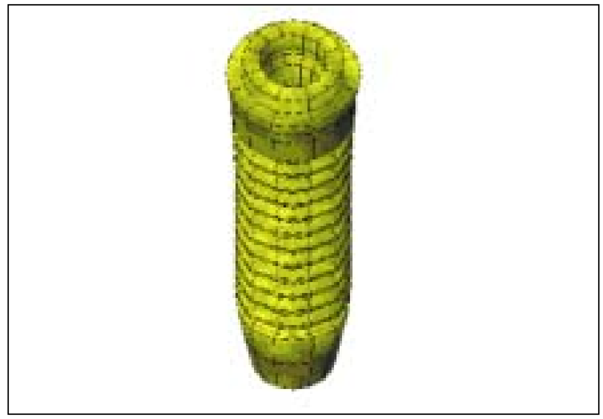

Fig 1b Finite element model of the cylindric implant, diameter = 3.75 mm, length = 11.5 mm.

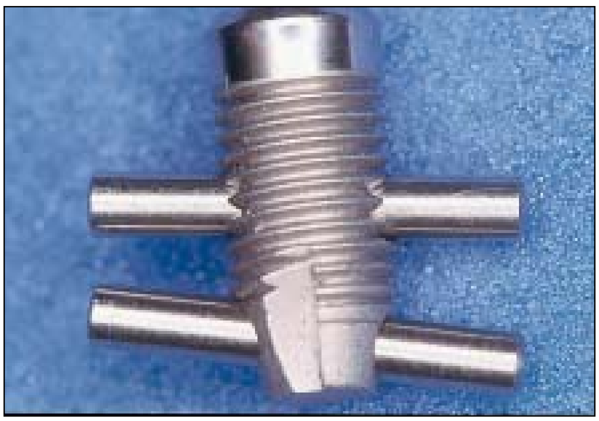

Fig 2a Implant with a locking pin system (Secure, Euroteknika).

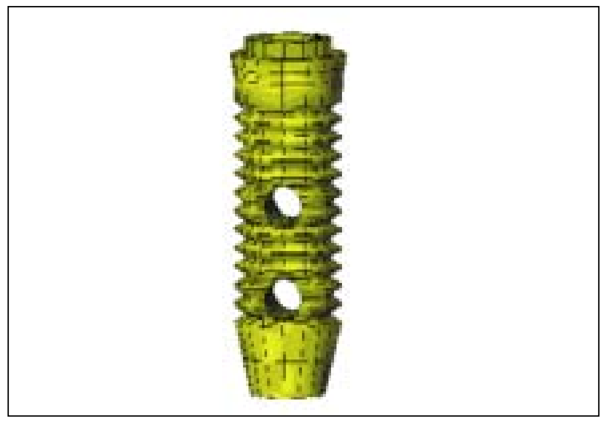

Fig 2b Finite element model of the locking pin implant, diameter = 3.75 mm, length = 11.5 mm.

Fig 3a *(Left)* Expanding implant in the non-expanded position (Diagnose, Euroteknika).

Fig 3b Finite element model of the expanding implant, cervical diameter = 3.75 mm, length = 11.5 mm, apical diameter = 6 mm.

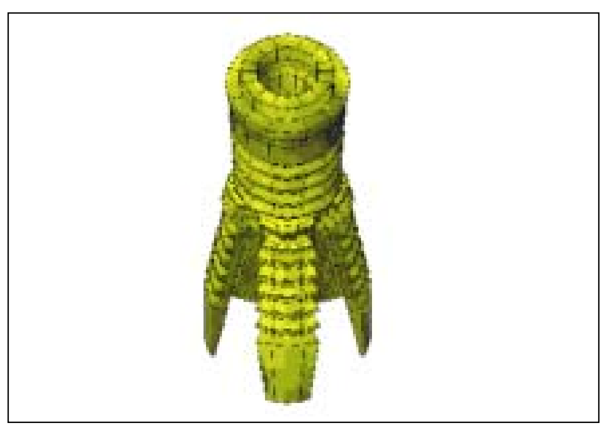

Figs 4a to 4c Buccolingual section view of the different types of implants.

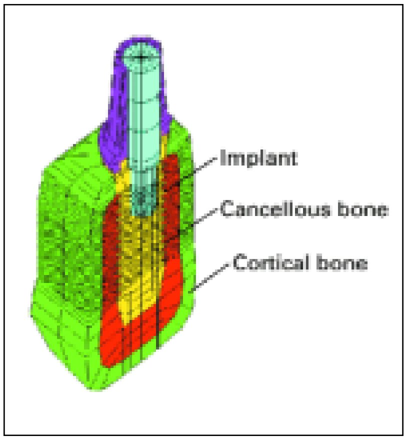

Fig 4a Cylindric implant (5,000 elements).

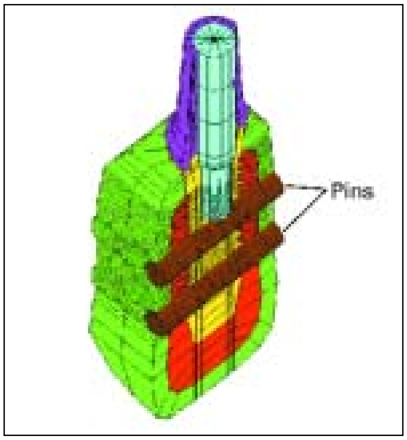

Fig 4b Locking pin implant (5,568 elements).

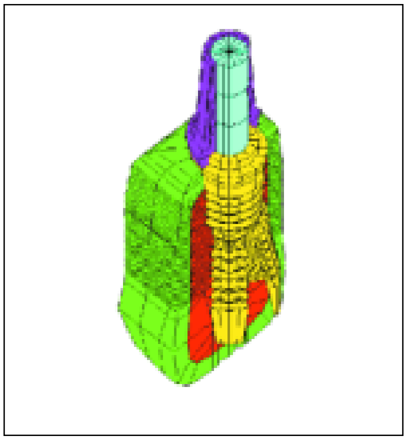

Fig 4c Expanding implant (7,008 elements).

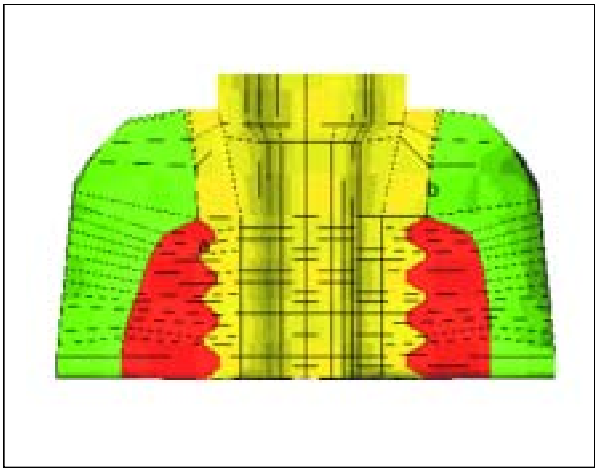

Fig 5 View of the bone-implant interface in the cervical region. Osseointegration (interfacial rigidity) is effective only in the initial part of the threading (a). A virtual membrane (b) limits interfacial rigidity.

Table 2 Mechanical Properties Used in the Study

		Cancellous bone			
	Titanium	Cb1	Cb2	Cb3	Cortical bone
Young's modulus (E)(GPa)	140	2.50	1.5	0.5	14
Poisson's ratio (ν)	0.3	0.3	0.3	0.3	0.35

Table 3 Displacements (in µm) for the 3 Implant Designs Under Different Load Directions, Related to the Cancellous Bone Characteristics

Load/ implant type	Cb1	Cb2	Cb3
Axial load			
Cylinder	4.187	5.269	8.013
Expanding	3.885	4.679	6.752
Locking pin	3.584	4.119	4.269
Oblique load (45 degrees)			
Cylinder	29.93	32.25	36.31
Expanding	29.89	32.07	35.65
Locking pin	28.82 (20.08)	30.55 (21.76)	30.60 (24.13)
Horizontal load			
Cylinder	39.38	41.96	45.81
Expanding	39.23	41.81	45.79
Locking pin	38.20 (28.17)	40.32 (29.00)	40.60 (29.99)

Parentheses indicate displacements for a horizontal load (at a right angle to the pins) following the mesiodistal direction.

Table 4 Percent Increases in the Implant Displacements Related to Bone Quality

Load/ implant type	Cb1	Cb2	Cb3
Cylinder			
Axial	—	+25.8%	+91.4%
45 degrees	—	+7.7%	+21.3%
90 degrees	—	+6.5%	+16.0%
Expanding			
Axial	—	+20.4%	+73.8%
45 degrees	—	+7.2%	+19.2%
90 degrees	—	+6.5%	+16.7%
Locking pin			
Axial	—	+14.9%	+19.9%
45 degrees BL	—	+6.0%	+6.1%
45 degrees MD	—	+8.4%	+20.0%
90 degrees BL	—	+5.5%	+6.2%
90 degrees MD	—	+2.9%	+6.4%

BL = buccolingual; MD = mesiodistal.

loss. Types I, II, and III bone provide good mechanical strength. Type IV bone has a thin cortex and poor medullary strength with low trabecular density.[35] Depending on the bone rigidity (high or low), the data exhibited are those of extreme maximal (cancellous bone 1 [Cb1], E = 2.5 GPa) or minimal (Cb3, 0.5 GPa) values. An intermediate value was also chosen (Cb2, E = 1.4 GPa). For all 3 bone types, Poisson's ratio = 0.3.[36,37] The program displayed displacements in all 3 directions of an orthonormal space (dy, dx, dz). Resultants of the displacements (ds) were collected for all 3 models at an arbitrarily chosen point at the neck of the implant. The von Mises stress intensities were recorded in the neck region of the implant.

RESULTS

For each implant design, the loading process generated immediate movement. The amplitude and direction of this movement depended on the direction of the load and the rigidity of the osseous base receiving the implant. The method previously described assumes that the implant is intimately in contact with the bone, thereby simulating osseointegration or the immediate stability clinically observed. Results appear in Table 3.

Relationship Between Implant Displacement and Cancellous Bone Quality

Under an axial load, and compared to the implant displacement in high-rigidity bone (E = 2.5 GPa) used as a reference, the displacement of implants set in intermediate-rigidity bone (E = 1.4 GPa) increased by 25.8% for the cylindric implant, by 20.4% for the apical expansion implant, and by 14.9% for the locking pin implant design. When bone rigidity was set to lowest values (E = 0.5 GPa), implant displacement increased by 91.4% for the cylindric implant, 73.8% for the expanding design, and by 19.9% for the locking pin design. Under oblique and horizontal loads, the influence was clearly weaker (Table 4).

Relationship Between Implant Displacement and Orientation of Applied Load

Implant displacement increased considerably as the direction of the load moved farther away from the implant main axis (Figs 6a to 6c). The influence of load orientation was stronger when bone rigidity was greater (E = 2.5 GPa). When compared to implant displacement under axial loads, the implant displacement under oblique loads (45 degrees) increased by 614% for the cylindric implant, by 669% for the apical expansion implant, and by 700% for the locking pin implant system. Again with the displacement under axial loads as a reference, the displacement under horizontal loads increased by 840% for the cylindric model, by 909% for the apical expansion model, and by 965% for the locking pin implant design. As bone rigidity decreased, implant displacement increased in the same order of magnitude. This indicates that displacement was greater when the load was applied horizontally.

Figs 6a to 6c Amount of displacement related to the load orientation.

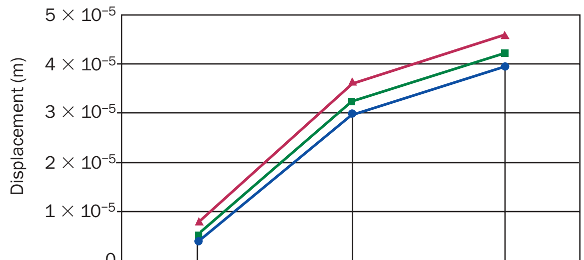

	Axial load	Load at 45 degrees	Horizontal load
Cb1	4.187×10^{-6}	2.993×10^{-5}	3.938×10^{-5}
Cb2	5.269×10^{-6}	3.225×10^{-5}	4.296×10^{-5}
Cb3	8.013×10^{-6}	3.631×10^{-5}	4.681×10^{-5}

Fig 6a Displacement of the cylindric implant.

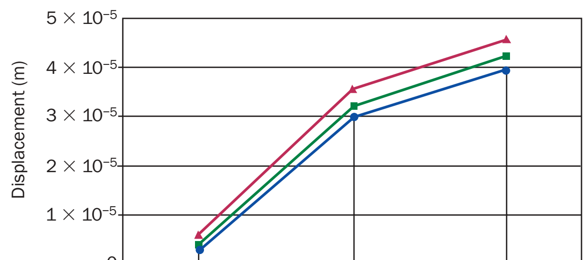

	Axial load	Load at 45 degrees	Horizontal load
Cb1	3.885×10^{-6}	2.989×10^{-5}	3.923×10^{-5}
Cb2	4.679×10^{-6}	3.207×10^{-5}	4.181×10^{-5}
Cb3	6.752×10^{-6}	3.565×10^{-5}	4.579×10^{-5}

Fig 6b Displacement of the expanding implant.

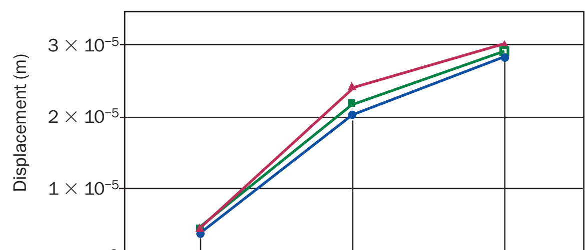

	Axial load	Load at 45 degrees	Horizontal load
Cb1	3.584×10^{-6}	2.008×10^{-5}	2.817×10^{-5}
Cb2	4.119×10^{-6}	2.176×10^{-5}	2.900×10^{-5}
Cb3	4.269×10^{-6}	2.413×10^{-5}	2.999×10^{-5}

Fig 6c Displacement of the locking pin implant.

Relationship Between Displacement and Implant Design

When the load was applied parallel to the implant axis, initial stability of the pin implant was clearly superior (Fig 7a). These displacements, when put under axial loads, compared to those recorded for the cylindric implant, decreased by 14% (0.6 μm) in high-rigidity bone (E = 2.5 GPa), 22% (1.15 μm) in intermediate-rigidity bone (E = 1.4 GPa), and 47% (3.7 μm) in low-rigidity bone (E = 0.5 GPa). With the cylindric threaded implant as a reference, the initial stability of the apical expansion implant was superior, but the difference was less important. The displacement under axial load decreased by 7% (0.3 μm) in rigid bone, 11% (0.6 μm) in intermediate-rigidity bone, and 16% (1.26 μm) in low-rigidity cancellous bone. When the load was oblique (at a 45-degree angle) (Fig 7b), the initial stability of the pin implant was clearly better, especially following the MD direction (perpendicular to the pins). Its displacements when put under oblique loads following the MD direction, compared to those of the

Figs 7a to 7c Histograms of the displacements for each implant under the different load directions in cancellous bone. Displacements are given in meters. Cb1: E = 2.5 GPa; Cb2: E = 1.4 GPa; Cb3: E = 0.5 GPa.

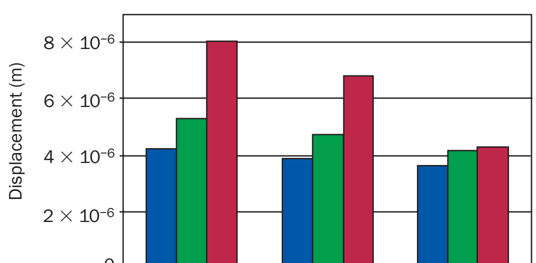

	Axial load	Apical expansion	Locking pin
Cb1	4.187×10^{-6}	3.885×10^{-6}	3.584×10^{-6}
Cb2	5.269×10^{-6}	4.679×10^{-6}	4.119×10^{-6}
Cb3	8.013×10^{-6}	6.752×10^{-6}	4.269×10^{-6}

Fig 7a Axial load.

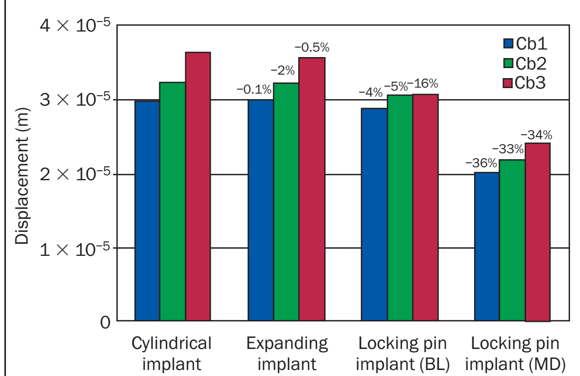

Fig 7b Oblique load.

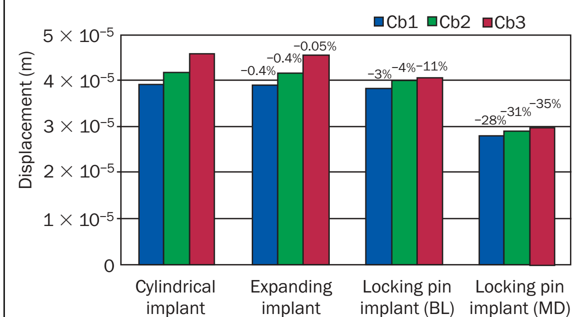

Fig 7c Horizontal load.

cylindric implant, were reduced by 33% (9.85 µm) in rigid cancellous bone, 36% (10.5 µm) in intermediate-rigidity bone, and 16% (1.26 µm) in low-rigidity cancellous bone. With the same cylindric implant as a reference, the initial stability of the apical expansion implant was superior, but the difference was very weak. The displacement under oblique loads (identical in the BL and MD directions) decreased by only 0.1% (0.04 µm) in the high-rigidity bone, by 0.5% (0.18 µm) in the medium-rigidity bone, and by 2% (0.6 µm) in the low-rigidity bone. When the load was horizontal (Fig 7c), initial stability of the locking pin implant was clearly better, particularly following the MD direction (perpendicular to pins). The displacement under horizontal loads, following the MD direction, compared to that recorded in cylindric implants, decreased by 28% (11.21 µm) in high-rigidity bone, by 31% (12.96 µm) in intermediate-rigidity bone, and by 35% (15.82 µm) in low-rigidity bone. With the cylindric threaded implant as a reference, the initial stability of the apical expansion implant was not clearly superior, regardless of the cancellous bone quality.

Relationship Between Cervical Stresses and Load Orientation

For each implant configuration investigated and regardless of the bone rigidity, the highest recorded stresses were those generated by horizontal forces. Figure 8 illustrates data obtained with low rigidity applied to the bone model.

Relationship Between Stress Distribution and Implant Design

Figures 9a to 9c represent the models put under an axial load. Iso-stress intensity ranges are represented in red and yellow. With the conventional cylindric threaded implant, results matched those of the literature and confirmed the importance of cervical stress. With the apical expansion implant (Fig 9b), stress distribution was less concentrated; stresses spread out evenly from neck to apex. With the pin implant (Fig 9c), stresses appeared concentrated around the pins.

Relationship Between Intensity of Cervical Stresses and Implant Design

In both configurations studied, reduction in the intensity of cervical shearing stresses (comparable to von Mises stresses) was measured. Whatever the load orientation, the conventional cylindric implant transmitted the highest stresses to the neck region of the implant. Under axial loads, stresses decreased by 75% (24 MPa) for the apical expansion implant and by 69% (22 MPa) for the pin implant. Under

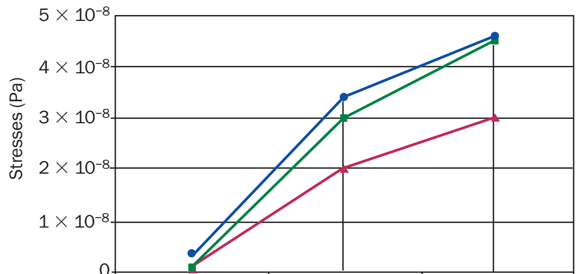

	Axial	45 degrees	90 degrees
Cylinder	3.230×10^7	3.400×10^8	4.600×10^8
Expanding	8.000×10^7	3.000×10^8	4.500×10^8
Locking pin	1.000×10^7	2.000×10^8	3.000×10^8

Fig 8 Shearing stresses (von Mises) increase related to the load orientation, as modeled in low-density cancellous bone (E = 0.5 GPa).

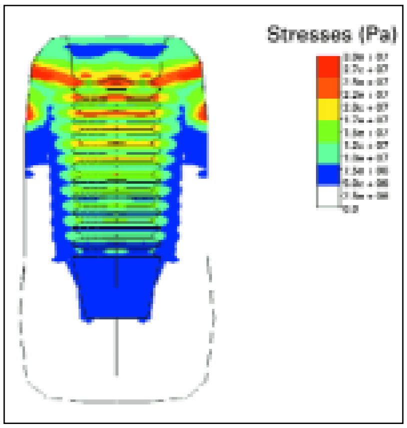

Fig 9a View of the shearing stresses on a cross section of cylindric implant set in the bony base.

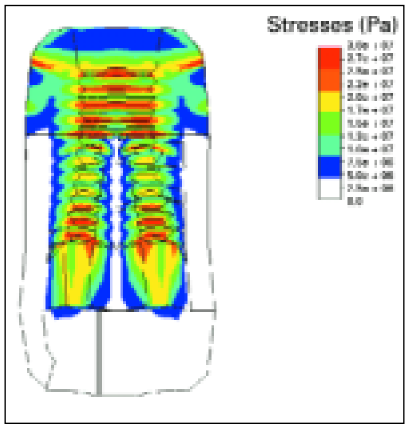

Fig 9b View of the shearing stresses on a cross section of the expanding implant set in the bony base.

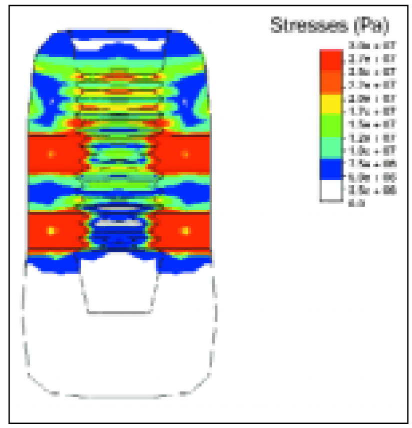

Fig 9c View of the shearing stresses on a cross section of the locking pin implant set in the bony base.

oblique loads, stresses decreased by 11.7% (40 MPa) for the apical expansion implant and by 41% (140 MPa) for the pin implant. Under horizontal loads, stresses generated in the 2 investigated implants decreased by 2.2% (10 MPa) for the apical expansion implant and by 35% (150 MPa) for the pin implant.

DISCUSSION

The aims of this study were to evaluate the influence of 2 implant designs compared to a standard cylindric implant in their control of micromovements and to determine the intensity and distribution of stresses after immediate loading by FEA. FEA is a computer-based numeric technique for calculating the strength and behavior of engineering structures. It can be used to calculate deflection, stress, vibration, buckling behavior, and many other phenomena. It can analyze elastic deformation or plastic deformation. The computer is required because of the considerable number of calculations needed to analyze a structure.

In the finite element method, a structure is broken down into many small simple blocks or elements. The behavior of an individual element can be described with a relatively simple set of equations. Just as the set of elements would be joined together to build the whole structure, the equations describing the behaviors of the individual elements are joined into an extremely large set of equations that describe the behavior of the whole structure. From the solution, the computer extracts the behavior of the individual elements. From this, it can calculate the stress and deflection of all the parts of the structure. The technique has been widely used in orthopedics for the design of hip prostheses.

The lack of initial postoperative implant stability (primary stability) is recognized as an important determinant in the loosening failure process of implants.[1,13] Physiologic loads giving rise to bone-implant relative micromovements of the order of 100 or 200 µm may inhibit bone ingrowth, resulting in the formation of a fibrous tissue layer, which then promotes loosening of the implant.[38,39] An accurate evaluation of the bone-implant relative micromotion is becoming important both in preclinical and clinical contexts. The preclinical validation of new prosthetic designs often involves evaluation of the primary stability by means of in vitro measurements, and FEA may be of considerable interest. In clinical practice, primary stability can be assessed intraoperatively by resonance frequency analysis, as proposed by Meredith and associates.[40]

The quality of cancellous bone strongly influences implant displacement, which increases as bone rigidity decreases. Under axial loads, the influence of cancellous bone rigidity is more important. However, the 2 implant configurations evaluated here—and more particularly the locking pin implant—minimized this influence. Under an axial load, the displacement of implants in bone with an intermediate rigidity increased by 25.8% for the cylindric implant and by 14.9% for the locking pin implant design (when compared to values obtained in bone with high rigidity). The displacement of implants in bone with the lowest rigidity increased by 91.4% for the cylindric implant and by 19.9% for the locking pin design. Whatever the implant type, this influence decreases as the direction of the load moves farther away from the main axis of the implant. The load orientation is a crucial parameter according to statements by several authors,[41–43] and it should be applied as closely as possible to the main axis of the implant. Whatever the bone rigidity, the pin implant exhibited more favorable behavior regarding changes in load orientation.

Results reported in the literature concerning the localization of stresses on an implant are very similar to the present data. Using FEA, several authors have found that the highest risk of bone resorption occurs in the neck region of an implant.[44–51] In comparison to the cylindric implant, it appears that the 2 investigated configurations would reduce the intensity of cervical stress. In the present study, stress intensities were decreased by 75% for the apical expansion implant under axial loads and by 11.7% under oblique loads. Stress intensities were decreased by 69% for the pin implant under axial loads and by 41% under oblique loads. Longitudinal MD sections (following the Y-Z plane) of the bone base, isolated from the rest of the model, demonstrated that both designs also modify the distribution of shearing stresses. In this study, it was found that stress distribution was less concentrated in the neck region with the apical expansion implant and the pin implant.

CONCLUSIONS

The first model tested was a bicortical pin implant and the second was an apical expansion implant. Regardless of the quality of the cancellous bone and the load orientation, initial stability of the pin implant was greater than that of the other investigated design. Initial stability of the apical expansion implant was higher than that of the reference cylindric implant, though the difference was small. Whatever the implant design and the cancellous bone quality, the highest stresses were observed when the load was imposed in the horizontal direction. The investigated configurations strongly influenced the distribution and the intensity of cervical shear stresses. The reference cylindric implant transmitted the highest stresses to the neck region of the implant. With the expanding implant, stress location was most favorable; the stresses were spread out evenly from the neck to the apical region. In contrast, cervical stresses appeared weaker with the pin implant, with the higher stresses concentrated around the pins.

ACKNOWLEDGMENTS

Authors are greatly indebted to Euroteknika (Paris, France), who helped in designing the new implant models.

REFERENCES

1. Albrektsson T, Brånemark P-I, Hansson HA, Lindstrom J. Osseointegrated titanium implants: Requirements for ensuring a long-lasting direct bone-to-implant anchorage in man. Acta Orthop Scand 1981;52:155–170.
2. Parr GR, Gardner LK, Toth RW. Titanium: The mystery metal of implant dentistry. Dental material aspect. J Prosthet Dent 1985;54:410–413.
3. Kasemo B. Biocompatibility of titanium implants: Surface science aspects. J Prosthet Dent 1983;49:832–837.
4. Haraldson T. A photoelastic study of some biomechanical factors affecting the anchorage of osseointegrated implants in the jaw. Scand J Plast Reconstr Surg 1980;14:209–214.
5. Carlsson L, Roslund T, Albrektsson T, Brånemark P-I. Osseointegration of titanium implants. Acta Orthop Scand 1986;57:285–289.
6. Quirynen M, Naert I, van Steenberghe D. Fixture design and overload influence marginal bone loss and fixture success in the Brånemark system. Clin Oral Implants Res 1992; 6:238–245.
7. Lavelle C, Wedgwood D, Love WB. Some advances in endosseous implants. J Oral Rehabil 1981;8:319–331.
8. Eriksson RA, Albrektsson T. Temperature threshold levels for heat-induced bone tissue injury: A vital microscopic study in the rabbit. J Prosthet Dent 1983;50:101–107.
9. Eriksson RA, Albrektsson T. The effect of heat on bone regeneration. J Oral Maxillofac Surg 1984;42:705–711.
10. Lekholm U. Clinical procedures for treatment with osseointegrated dental implants. J Prosthet Dent 1983;50:116–120.

11. Schroeder A, Zypen E, Stich H, Sutter F. The reaction of bone, connective tissue, and epithelium to endosteal implants with titanium-sprayed surface. J Maxillofac Surg 1981;9:15–25.
12. Heimke G, Schulte W, d'Hoedt B, Griss P, Busing CM, Stock D. The influence of fine surface structures on the osseointegration of implants. Int J Artif Organs 1982;3:207–212.
13. Albrektsson T, Dahl E, Enbom L, et al. Osseointegrated oral implants. A Swedish multicenter study of 8139 consecutively-inserted Nobelpharma implants. J Periodontol 1988; 59:287–296.
14. Anneroth G, Hedstrom KG, Kjellman O, Kondell PA, Norderam A. Endosseous titanium implants in extraction sockets: An experimental study in monkeys. Int J Oral Surg 1985;14:50–54.
15. Babbush CA, Kent JN, Misiek DJ. Titanium plasma-sprayed (TPS) screw implants for the reconstruction of the edentulous mandible. J Oral Maxillofac Surg 1986;44:274–282.
16. Ten Bruggenkate CM, Muller K, Oosterbeek HS. Clinical evaluation of the ITI (F-type) hollow cylinder implant. Oral Surg Oral Med Oral Pathol 1990;70:693–697.
17. Buser D, Weber HP, Bragger U, Balsiger C. Tissue integration of one-stage ITI implants: 3-year results of a longitudinal study with hollow-cylinder and hollow-screw implants. Int J Oral Maxillofac Implants 1991;6:405–412.
18. Becker W, Becker BE, Israelson H, et al. One-step surgical placement of Brånemark implants: A prospective multicenter clinical study. Int J Oral Maxillofac Implants 1997;12:454–462.
19. Roynesdal AK, Ambjornsen E, Haanaes HR. A comparison of 3 different endosseous nonsubmerged implants in edentulous mandibles: A clinical report. Int J Oral Maxillofac Implants 1999;14:543–548.
20. Brunski JB. Biomechanical factors affecting the bone-dental implant interface. Clin Mater 1992;10:153–201.
21. Brunski JB. Avoid pitfalls of overloading and micromotion of intraosseous implants. Dent Implant Update 1993;4:77–81.
22. Schnitman PA, Wohrle PS, Rubenstein JE. Immediate fixed interim prostheses supported by two-stage threaded implants: Methodology and results. J Oral Implantol 1990;16:96–105.
23. Schnitman PA. Brånemark implants loaded with fixed provisional prostheses at fixture placement: Nine-year follow-up . J Oral Implantol 1995;21:235.
24. Lum LB, Beirne OR, Curtis DA. Histological evaluation of hydroxyapatite-coated versus uncoated titanium blade implants in delayed applications. Int J Oral Maxillofac Implants 1991;6:456–462.
25. Sagara M, Akagawa Y, Nikai H, Tsuru H. The effect of early occlusal loading on one-stage titanium alloy implants in beagle dogs: A pilot study. J Prosthet Dent 1993;69:281–288.
26. Salama H, Rose LF, Salama M, Betts NJ. Immediate loading of bilaterally splinted titanium root-form implants in fixed prosthodontics—A technique reexamined: Two case reports. Int J Periodontics Restorative Dent 1995;15:345-361.
27. Tarnow DP, Emtiaz S, Classi A. Immediate loading of threaded implants at stage 1 surgery in edentulous arches: Ten consecutive case reports with 1 to 5 year data. Int J Oral Maxillofac Implants 1997;12:319–324.
28. Gomes A, Lozada JL, Caplanis N, Kleinman A. Immediate loading of a single hydroxyapatite-coated threaded root form implant: A clinical report. J Oral Implantol 1998;24:159–166.
29. Weinberg LA. Reduction of implant loading with therapeutic biomechanics. Implant Dent 1998;7:277–285.
30. Hure G, Donath K, Lesourd M, Chappard D, Baslé MF. Does titanium surface treatment influence the bone-implant interface? SEM and histomorphometry in a 6-month sheep study. Int J Oral Maxillofac Implants 1996;11:506–511.
31. Craig RG. Restorative Dental Materials, ed 9. London: Mosby-Year Book, 1993.
32. Meroueh K, Watanabe F, Mentag P. Finite element analysis of partially edentulous mandible rehabilitated with an osseointegrated cylindrical implant. J Oral Implantology 1987;2:215–238.
33. Borchers L, Reichart P. Three-dimensional stress distribution around a dental implant at different stages of interface development. J Dent Res 1983;62:155–159.
34. De Vree JH, Peters MC, Plasschaert AJ. A comparison of photoelastic and finite element stress analysis in restored tooth structures. J Oral Rehabil 1983;10:505–517.
35. Jaffin RA, Berman CL. The excessive loss of Brånemark fixtures in type IV bone: A 5-year analysis. J Periodontol 1991; 62(1):2–4.
36. Farah JW, Craig RG, Eden GT, Grossman DG. Two-dimensional photoelastic simulation of a castable ceramic fixed partial denture. J Prosthet Dent 1988;59:8–12.
37. Cook SD, Klawitter JJ, Weinstein AM. The influence of implant elastic modulus on the stress distribution around LTI carbon and aluminum oxide dental implants. J Biomed Mater Res 1981;15:879–887.
38. Pilliar RM, Lee JM, Maniatopoulos C. Observations on the effect of movement on bone ingrowth into porous-surfaced implants. Clin Orthop 1986;208:108–113.
39. Viceconti M, Muccini R, Bernakiewicz M, Baleani M, Cristofolini L. Large-sliding contact elements accurately predict levels of bone-implant micromotion relevant to osseointegration. J Biomech 2000;33:1611–1618.
40. Meredith N, Book K, Friberg B, Jemt T, Sennerby L. Resonance frequency measurements of implant stability in vivo. A cross-sectional and longitudinal study of resonance frequency measurements on implants in the edentulous and partially dentate maxilla. Clin Oral Implants Res 1997;8:226–233.
41. Weinberg LA. The biomechanics of force distribution in implant-supported prostheses. Int J Oral Maxillofac Implants 1993;8:19–31.
42. Misch CE, Bidez MW. Implant-protected occlusion: A biomechanical rationale. Compendium 1994;15:1330–1334.
43. Holmgren EP, Seckinger RJ, Kilgren LM, Mante F. Evaluating parameters of osseointegrated dental implants using finite element analysis—A two-dimensional comparative study examining the effects of implant diameter, implant shape and load direction. J Oral Implantol 1998;24:80–88.
44. Lozada JL, Abbate MF, Pizzarella FA, James RA. Comparative three-dimensional analysis of two finite element endosseous implant designs. J Oral Implantol 1994;20:315–321.
45. Matsushita Y, Kitoh M, Mizuta K, Ikeda H, Suetsugu T. Two-dimensional FEM analysis of hydroxyapatite implants: Diameter effects of stress distribution. J Oral Implantol 1990;16:6–11.
46. Rieger MR, Mayberry M, Brose MO. Finite element analysis of six endosseous implants. J Prosthet Dent 1990;63:671–676.
47. Clelland NL, Ismail YH, Zaki HS, Pipko D. Three-dimensional finite element stress analysis in and around the Screw-Vent implant. Int J Oral Maxillofac Implants 1991;6:391–398.
48. Clift SE, Fisher J, Watson CJ. Finite element stress and strain analysis of the bone surrounding a dental implant: Effect of variations in bone modulus. Proc Inst Mech Fug 1992;206:233–241.
49. Meijer HI, Kuiper JH, Starmans FJM, Bosman F. Stress distribution around dental implants: Influence of superstructure, length of implant and height of mandible. J Prosthet Dent 1992;68:96–102.
50. Meijer HI, Starmans FJ, Steen WH, Bosman F. Loading conditions of endosseous implant in an edentulous human mandible: Three-dimensional finite element study. J Oral Rehabil 1996;23:757–763.
51. Weinberg LA, Kruger B. Biomechanical considerations when combining tooth-supported and implant-supported prostheses. Oral Surg Oral Med Oral Pathol 1994;78:22–27.